Tetrahedron: *Asymmetry* xxx (2017) xxx–xxx

Contents lists available at ScienceDirect

Tetrahedron: *Asymmetry*

journal homepage: www.elsevier.com/locate/tetasy

Synthesis and crystal structure of a chiral lactam and three amino alcohols as potential protein tyrosine phosphates 1B inhibitors

Şafak Özhan Kocakaya [a], Mehmet Karakaplan [a,*], Rosario Scopelliti [b]

[a] *Department of Chemistry, Faculty of Science, Dicle University, 21280 Diyarbakır, Turkey*
[b] *Ecole Polytechnique Fédérale de Lausanne (EPFL), CH-1015 Lausanne, Switzerland*

ARTICLE INFO

Article history:
Received 30 June 2017
Revised 5 September 2017
Accepted 15 September 2017
Available online xxxx

Dedicated to the memory of Dr. Howard Flack

ABSTRACT

Chiral lactam **2** and three chiral β-amino alcohols **3**–**5** have been synthesized and characterized by spectroscopic techniques. Regioselective ring opening reaction of chiral styrene oxide by an amine nucleophile was confirmed by X-ray diffraction data. Ligand **2**–**4** crystallizes in the tetragonal, orthorhombic and tetragonal crystal lattice system respectively. Ligands **2**–**6** have been used as potential inhibitors for protein tyrosine phosphatase 1B enzyme (PTP1B). The potential inhibitor effect of these molecules to the target protein was investigated by Dock and molecular dynamics calculations. Dock score analysis and Lipinski parameters suggested that ligands **1**, **2**, **4**–**6** are potential inhibitors towards PTP1B, thus indicating that the residues Arg24, Arg254 and Met258, Asp29 in the second active site of PTP1B are essential for the high selectivity of inhibitors. The results indicate that the polar hydrogen bonding interacts with Asp29, Gln102, and the amino acid residues of PTP1B are responsible for governing inhibitory potency of ligands **1**–**6**.

1. Introduction

Protein tyrosine phosphatase 1B (PTP1B) is an intracellular protein expressed in insulin responsive tissues including the classical insulin targeted tissues such as liver, muscle and fat.[1] PTP1B plays an important role in insulin receptor signaling.[2] PTP1B dephosphorylates the insulin receptor during its biosynthesis in endoplasmic reticulum as well as after it has been stimulated by the insulin, and thus plays a central role in the negative regulation of the insulin signalling pathway.[3] Studies on mice have shown that insulin sensitivity and obesity correspond with an increase in PTP1B enzyme deficiency. Several experiments have also demonstrated that the knockout of PTP1B in mice can result in insulin hypersensitivity, even in a high-fat diet.[4–9]

Therefore, small molecular inhibitors of PTP1B are promising drugs for potentially curing type II diabetes. The full length of PTP1B comprises of 435 amino acids, constituting the major cellular form; however, only a shorter length of 298 or 321 residues is typically considered in biochemical studies. The model used herein is the one coded 1wax.pdb in the protein Data Bank which contains 298 amino acids. The active site of PTP1B consists of residues His214-Arg221 and loops WPD (Thr177-Pro185), R (Val113-Ser118). The other important parts of PTP1B are S loops (Ser201-Gly209), R3-helix (Glu186-Glu200), R6-helix (Ala264-Ile281), and R7-helix, (Val287-Ser295) which take part in the catalysis substrate binding.[10–15] The second binding active site, close to the conserved primary active site, also referred to as site B, which was determined by Zhang et al., is not so conserved, and therefore it is believed that it should be exploited in the design PTP1B enzyme inhibitors with good selectivity.[6]

The design of small molecules that can inhibit the PTP1B enzyme is an area of research that has raised considerably interest in the medicinal chemistry field and is being actively pursued by many academic and industrial organizations. In clinical trials, the association between insulin resistance and PTP1B levels in fat and muscle tissues has been determined. A variety of PTP1B inhibitors have been reported over the last decade.[16–22] The discovery of potent, selective, cell permeable and orally bioavailable PTP1B inhibitors is a challenging medicinal chemistry objective. Out of several small molecule PTP1B inhibitors, only three small molecule PTP1B inhibitors have entered clinical trials and finally discontinued due to insufficient efficacy and unwanted side effects.[23]

The synthesis of new chiral ligands is the subject of ongoing scientific research.[24–26] The common route to β-amino alcohol ligands is the ring-opening reaction of epoxides by amines.[27–31] The outcome of the ring-openings strongly depends on the electronic and steric effects on reactants. Concerning the regioselectivity, the favoured product is the result of nucleophilic attack at the less

* Corresponding authors. Tel.: +90 4122488550.
E-mail addresses: safakozhan@dicle.edu.tr (Ş. Özhan Kocakaya), mkkaplan@dicle.edu.tr (M. Karakaplan).

https://doi.org/10.1016/j.tetasy.2017.09.014
0957-4166/

hindered epoxide carbon (β-attack), except in the case of styrene oxide, where an α-attack was the major one.[32] Concerning the stereochemistry, under neutral or basic conditions, an S_N2 mechanism was operating to *trans*-β-amino alcohols.

The identification of selective, safe and readily available inhibitors of these PTP1B has proven difficult and it still represents a challenge for medicinal chemists. Herein we report the synthesis of a lactam and five β-amino alcohols derived from (*R*,*R*)-1,2-diaminocyclohexane as potential PTP1B inhibitors (Scheme 1). Molecular modelling was used to understand the possible binding mode of proposed compounds.

2. Computational section

2.1. Molecular dynamics simulations

The ligands were then applied with partial atomic charges derived by fitting Antechamber obtained by electronic structure calculation module in AMBER and assigned the AM1-BCC charges.[33–36] Atoms on PTP1B were assigned the PARM99 charges, and all ionisable residues were set at their default protonation states at neutral pH. Parameters for the ligands were generated using XLEAP the general amber force field (GAFF).[37] Molecular Dynamics runs were in general for 1 ns at 300 K.

The coordinates of the protein mentioned above were taken from the Protein Data Bank (1wax PDB). Crystallographic water molecules were removed from all the structures. In 1wax.pdb, the missing coordinates were modelled using XLEAP and a ff99SB force field. Atoms on PTP1B were assigned the PARM99 charges, and all ionizable residues were set at their default protonation states at neutral pH. All structures were further processed by the xLeAP module of AMBER. The molecular systems were neutralized by the addition of counterions. The systems and then the energy were minimized in two steps; in the first step, the protein and ligand were kept fixed, only the water molecules were allowed to move, and in the second step, all atoms were allowed to move. For the first step, the energy minimization was performed in 500 and 2500 steps with the steepest descent and conjugate gradient methods, respectively. For the second step, the energy minimizations were performed in 500 and 2500 steps using the steepest descent and conjugant gradient methods, respectively.

2.2. Molecular docking

Dock 6.0 module allows all stages of a docking process to be performed with the generation of ligand conformations, ligand docking, and the scoring of the binding modes. As in this case, where a rigid receptor approximation was used, it is expected that the different receptors considered will lead to different ligand-binding modes depending on the initial size of the PTP1B-binding cavity. Thus, the six new PTP1B inhibitors were docked on the available receptor following a multistep procedure. In order to describe receptor-binding properties, a grid of potential energy was calculated for atoms taking part in the binding pocket. These atoms were obtained from the analysis of each protein–ligand complex. In this step, default parameters were used. The ligand was then docked using the calculated grid to place it into the cavity and score the proposed binding modes.

3. Results and discussions

The chiral unit of 1,2-diaminocyclohexane has the most suitable geometry parameters and commercial availability; therefore it is the one of the most important parts of the ligand structure.[38,39] Chiral ligands **2**–**5** were synthesized by starting from *cis*/*trans* mixtures of 1,2-diaminocyclohexane. The structures of all compounds were ambiguously assigned by means of analytical and spectroscopic data. The absolute configurations of compound **2**–**4** were assigned by X- ray crystallographic data (Figs. 1–3).

The known ligand **1** was prepared by the condensation of benzaldehyde and (*R*,*R*)-1,2-diaminocyclohexane obtained from classical resolution of *cis*/*trans* mixtures of 1,2-diaminocyclohexane to form an imine intermediate.[40] These intermediates were reduced by $NaBH_4$ to afford the desired ligand. Lactam **2** was easily prepared from ligand **1** and oxalyl chloride in 71% yield. The atom numbering scheme of **2** drawn at the 50% probability level is given in Figure 1. Lactam **2** crystallized into a tetragonal crystal lattice system with space group $P4_12_12$ (Table 1). The crystal packing of C_2 symmetric lactam **2** contains one ethanol molecule having hydrogen bonds with the carbonyl oxygen of lactam **2**. Bond distances N(1)—C(1) and N(2)—C(2) are 1.356 and 1.350 Å respectively. These bond lengths are shorter than those in amino alcohols

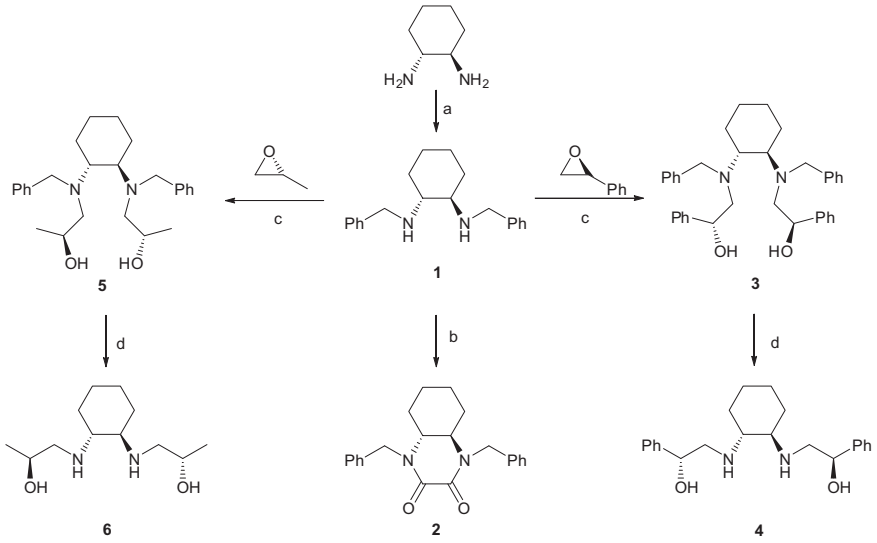

Scheme 1. Reagents: (a) PhCHO/MeOH than $NaBH_4$, (b) Oxalyl chloride, (c) $Pd(OH_2)/C$, [H_2].

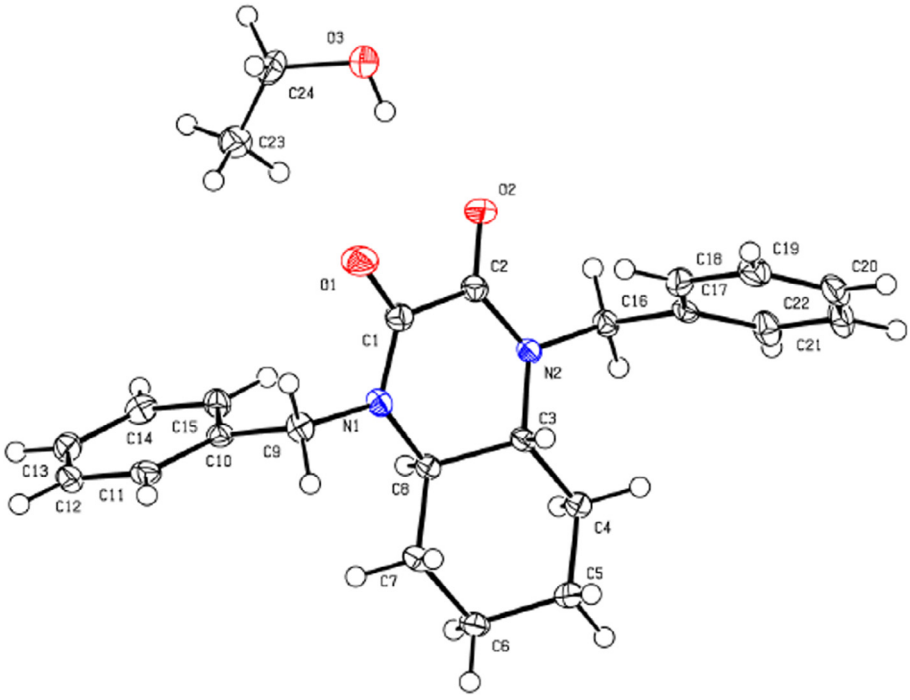

Figure 1. ORTEP diagram of the lactam **2**. Ellipsoids are shown at the 50% probability threshold.

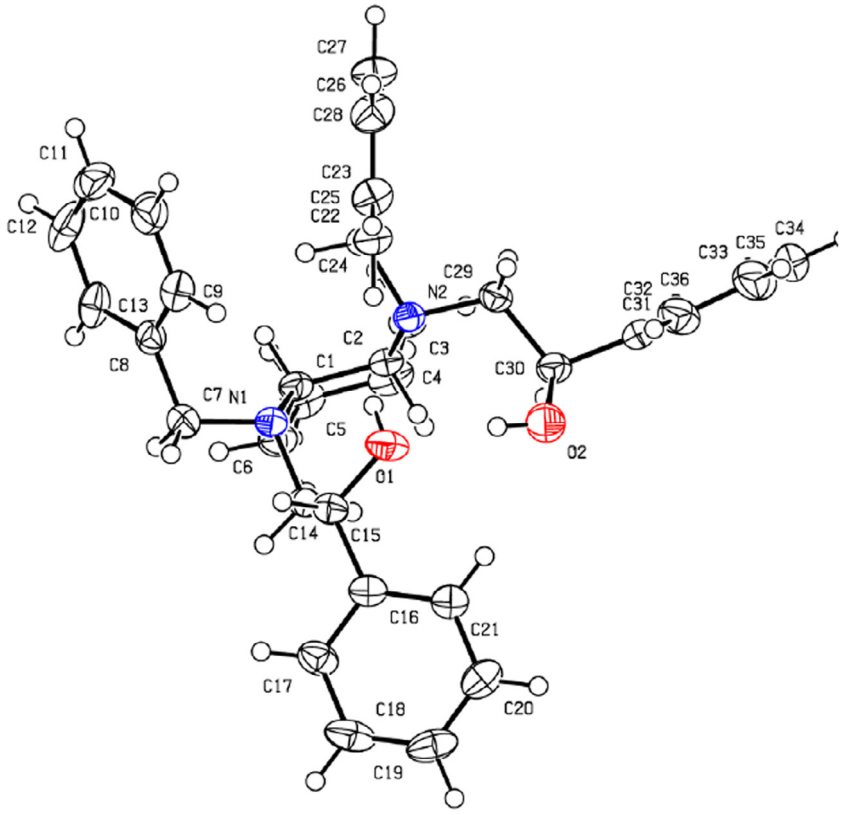

Figure 2. ORTEP plot of amino alcohol **3**. Ellipsoids are shown at the 50% probability threshold.

3 and **4**, which depend on the symmetrical electron withdrawing of carbonyl groups with bond lengths 1.2206 and 1.2246 Å. It has been shown that the lactam ring is planar; the C(1)—N(1)—C(8) and C(2)—N(2)—C(3) bond angels are 121.05 and 119.62°, respectively. The bond angels indicate that the cyclohexyl ring is in the chair confirmation and both stereogenic centers are (*R*)-configurations.

Epoxides are small molecules with a wide range of synthetic applications as intermediates in the pharmaceutical and agrochemical industries. It is susceptible to attack by a range of

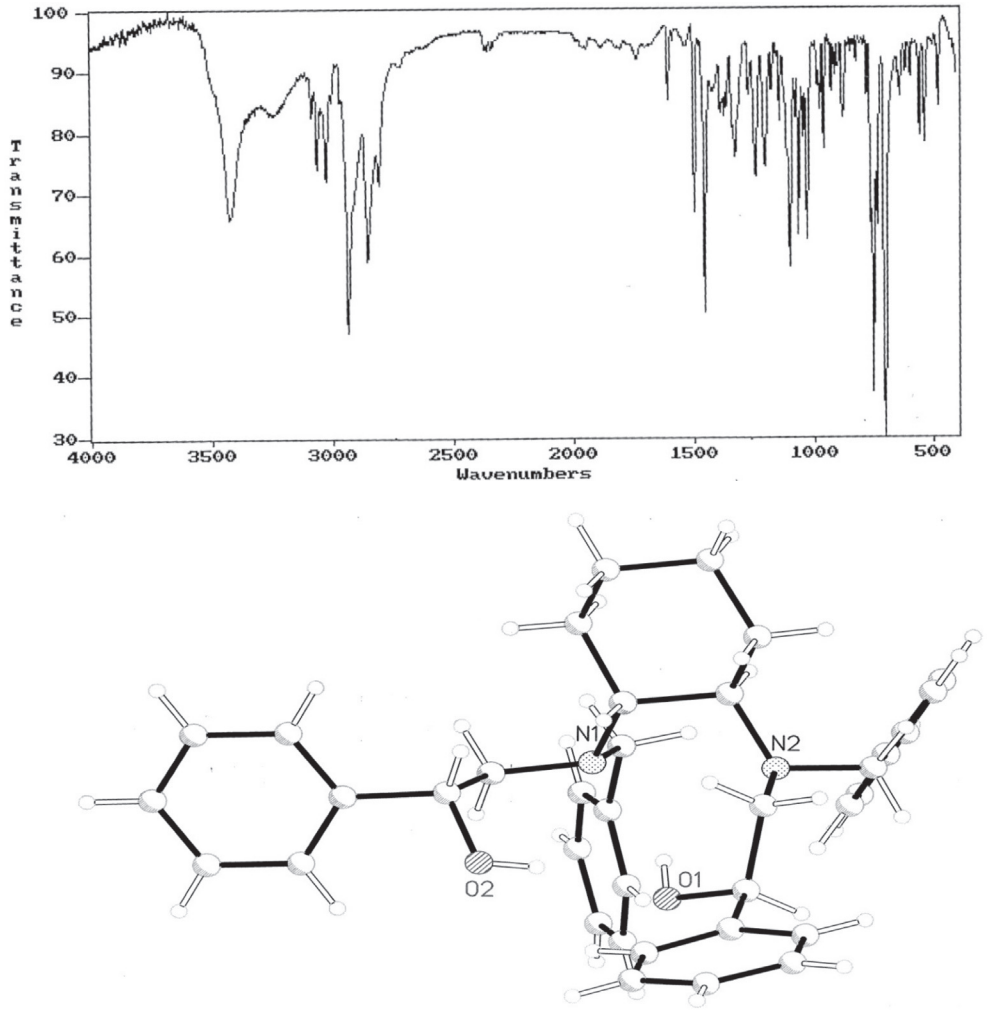

Figure 3. IR spectrum and ball-and-stick view of chiral amino alcohol **3**.

Table 1
Crystal data and structure refinement details for ligands **2**–**4**

	2		**3**		**4**	
Formula, formula weight	$C_{23}H_{27}N_2O_{2.5}$, 371.47		$C_{36}H_{42}N_2O_2$, 534.72		$C_{22}H_{30}N_2O_2$, 354.48	
Temperature	100(2) K		140(2) K		140(2) K	
Radiation	0.71073 Å		0.71073 Å		0.71073 Å	
Crystal system, space group	Tetragonal, $P4_12_12$		Orthorhombic, $P2_12_12_1$		Tetragonal, $P4_3$	
Unit cell dimensions	a = 10.1214(9) Å	α = 90°	a = 10.6029(4) Å	α = 90°	a = 11.364(3) Å	α = 90°
	b = 10.1214(9) Å	β = 90°	b = 16.0647(6) Å	β = 90°	b = 11.364(3) Å	β = 90°
	c = 37.475(7) Å	γ = 90°	c = 17.4065(8) Å	γ = 90°	c = 16.250(10) Å	γ = 90°
Volume (Å^3)	3839.0(8) Å^3		2964.9(2) Å^3		2098.5(8) Å^3	
Z, density (g/cm^3)	8, 1.285 Mg/m^3		4, 1.198 Mg/m^3		4, 1.122 Mg/m^3	
Absorption coefficient μ (m^{-1})	0.084 mm^{-1}		0.073 mm^{-1}		0.072 mm^{-1}	
F (000)	1592		1152		768	
Crystal size (mm)	0.44 × 0.40 × 0.29 mm^3		0.34 × 0.32 × 0.21 mm^3		0.32 × 0.25 × 0.22 mm^3	
Theta range	3.28–27.49°		3.03–28.79°		2.53–24.48°	
Index ranges	$-12 \le h \le 13$, $-13 \le k \le 13$,		$-14 \le h \le 14$, $-20 \le k \le 21$,		$-13 \le h \le 13$, $-13 \le k \le 13$,	
Index ranges	$-48 \le l \le 48$		$-22 \le l \le 23$		$-18 \le l \le 17$	
Reflection collected/unique	65,734		29,766		3376	
Independent reflections	4401 [R(int) = 0.0270]		7226 [R(int) = 0.0435]		3376 [R(int) = 0.0000]	
Completeness to theta = 24.48°	99.7%		99.8%		99.2%	
Absorption correction	Semi-empirical from equivalents		Semi-empirical from equivalents		None	
Refinement method	Full-matrix least-squares on F^2		Full-matrix least-squares on F^2		Full-matrix least-squares on F^2	
Data/restraints/parameters	4401/0/264		7226/0/369		3376/1/252	
Goodness-of-fit on F^2	1.127		1.026		1.131	
Final R indices [$I > 2\sigma(I)$]	R1 = 0.0344, wR2 = 0.0845		R1 = 0.0428, wR2 = 0.0817		R1 = 0.0486, wR2 = 0.0914	
R indices (all data) data]	R1 = 0.0371, wR2 = 0.0868		R1 = 0.0628, wR2 = 0.0898		R1 = 0.0600, wR2 = 0.0954	
Absolute structure parameter	−0.1(10)		−0.6(11)		2.2(14)	
Largest diff. peak and hole	0.232 and −0.202 e Å^{-3}		0.154 and −0.189 e Å^{-3}		0.147 and −0.146 e Å^{-3}	

Please cite this article in press as: Özhan Kocakaya, Ş; et al. *Tetrahedron: Asymmetry* (2017), https://doi.org/10.1016/j.tetasy.2017.09.014

nucleophiles, including nitrogen, oxygen, and sulfur containing compounds, leading to bifunctional molecules of great industrial value. Chiral amino alcohol **3** was synthesized by ring opening of (*R*)-styrene oxide with amine nucleophile **1** in a catalyst free medium using methanol. Although the synthesis of compound **3** was reported, its solid state form has not been reported so far.[41]

A single crystal of compound **3** was obtained as a bright colourless crystal by dissolving the crude product in *n*-hexane and a few drops of ethanol at room temperature. Its crystallographic image provides evidence to the regioselectivity about the attack of amine nucleophile to the styrene oxide. It showed that compound **3** is formed by a β-attack of nucleophile to the less hindered terminal carbon of styrene oxide without any racemisation (Fig. 2).

The IR spectrum of amino alcohols **3** also showed a free hydroxyl absorption band at approximately 3429 cm^{-1} (Fig. 3). This point was clarified by the crystallographic image of this compound. As can be seen from Figure 3, one of the phenyl ring of benzyl groups bearing to the nitrogen atom inhibits the formation of intramolecular hydrogen bonds between hydroxyl groups. Through X-ray crystal structure analysis, amino alcohol **3** crystallized into an orthorhombic crystal lattice system with space group $P2_12_12$ (Table 1).

Amino alcohol **4** with a secondary amine functionality was obtained by debenzylation of compound **3** with $Pd(OH)_2/C$ in high yields (70%). As can be seen from Figure 4, diastereomer of amino alcohol **4** crystallized into a tetragonal crystal lattice system with space group $P4_3$ (Table 1). The cyclohexyl ring is in a chair confirmation and has a (1*S*,1*S*)-configuration (Fig. 4). This was attributed to the enantiomeric impurity of compound **1**. Consequently, the structures of compound **2**–**4** derived from chiral 1,2-diaminocyclohexane were evaluated by their single crystal forms. In order to investigate the effect of a substituent on the second stereogenic center bearing a hydroxyl functional group, we designed chiral ligands **5** and **6**.

The 1,2-diamino moiety of ligands was selected in order to improve the stability of the inhibitor/enzyme complex through contacts with residues bearing a hydroxyl active site, which suggested a marked influence on the potential potency and selectivity. Molecular docking experiments into the PTP1B active site indicate that the 1,2-diamino moiety of compounds **2**–**6** fitted the binding site very well by establishing favourable polar and hydrogen bonding. All compounds showed similar interaction modes of binding in the second active site of PTP1B (Fig. 5).

With regards to the potential inhibitory effectiveness, PTP1B was shown to be enhanced by the apolar interactions of ligands investigated. The potential of the inhibitors is mainly governed by hydrophobic interactions, van der Waals contacts of the inhibitors with the Arg24, Arg257, Met258, Arg254, and Phe182 and hydrogen bonding. The calculated thermodynamic parameters for the complexation of (1*R*,2*R*)-1,2-diaminocyclohexane derivatives **1**–**6** by Docking method analysis are shown in Table 2. The energy of complexation was observed in the range from −16.98 to 42.22 kcal/mol, respectively. The orientations of these potential inhibitors in the enzyme B site indicate that the interaction of the hydrogen bond is of great importance during binding. In generally, the hydrogen bonds place the amine and hydroxyl functional groups of ligands between the Gln102 and Asp29 residues of the protein as shown in Figure 6.

The lactam functionality of ligand **2** has better calculated enzyme inhibitor properties than the more flexible ligand **1**. It is thought that the fixed geometry of ligand **2** would infer a powerful ability to bind with the target enzyme via apolar and polar interactions (Fig. 6). The hindrance of benzyl group on nitrogen atom of ligand **3** would make it less effective than ligand **4**, having a high total enclosed volume, occupying effectively van der Waals contacts of by Lys58, His60, Gln102 together with hydrogen bonds.

The similar chemical structures and stereochemistry of ligands **5** and **6** make them better potential inhibitors when compared with ligand **3** (Table 2). This was attributed to their lower lipophilic or more hydrophilic character. It was also found that the residues adjacent to the second active site of PTP1B, including Asp29, Arg24, Arg254, and Met258, might be partially responsible for the potential high inhibition activity and selectivity of ligand **6** by analyzing their interactions.

The potential inhibitor effect of ligands **1**–**6** has also been investigated by using calculated Lipinski parameters (Table 3). The results indicate that five of the ligands have a powerful enzyme inhibitor potent. These results are agreement with the literature.[42,43] Ligand **3** showed the lowest potential inhibitor efficiency for PTP1B due to the higher molecular weight, rotation bonds and log*P* value, as shown in Table 3.

Lipinski values have been supported Dock Score results showed that ligands **1**, **2** and **4**–**6** have a good potential inhibitor efficiency toward PTP1B enzyme.

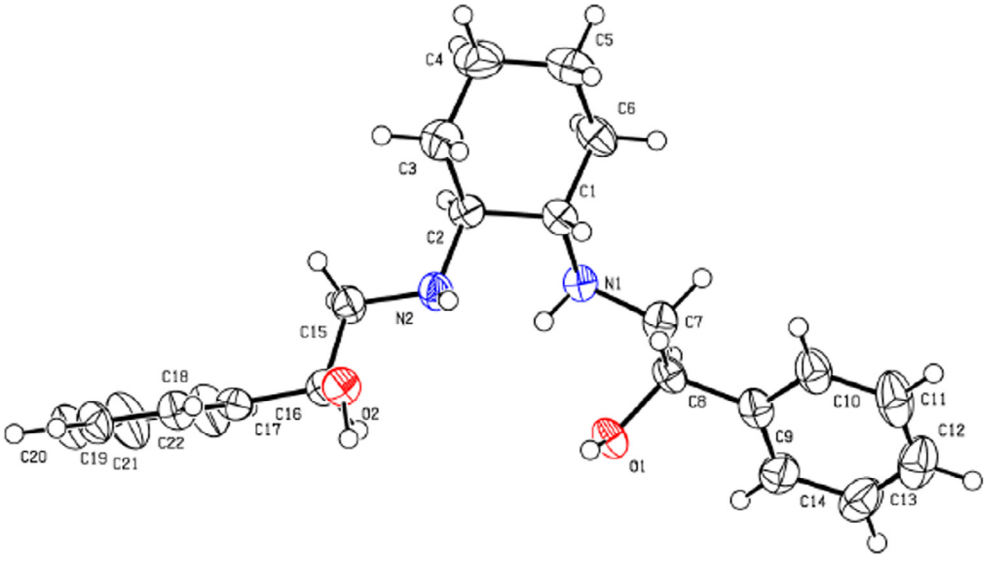

Figure 4. ORTEP diagram of diastereomer of chiral amino alcohol **4**. Ellipsoids are shown at the 50% probability threshold.

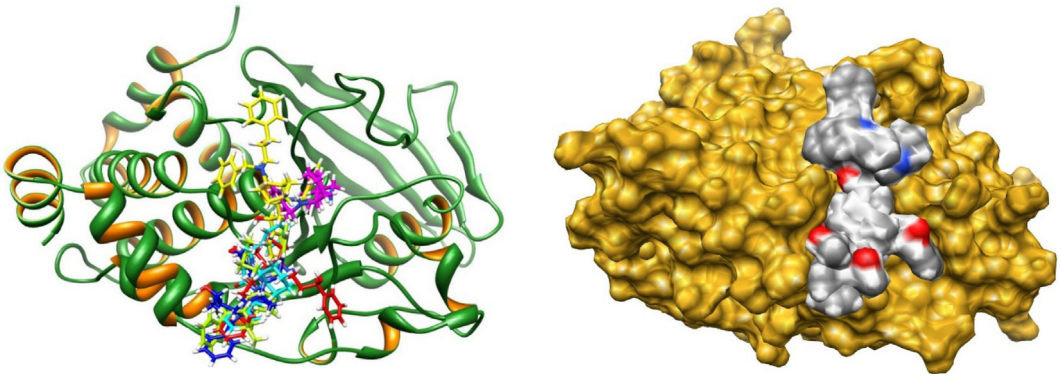

Figure 5. (A) Docking results of potential ligands **2**–**6** in the PTP1B catalytic pocket. Ligand **1**–**6** are coloured in pink, cyan, yellow, red, blue and green respectively. (B) Docking results of ligand **1**–**6** in the PTP1B second active site.

Table 2
Calculated thermodynamic parameters for complexation of ligands **1**–**6** as potential inhibitors for PTP1B by docking method

Ligand	Electrostatic energy	van der Waals energy	Dock score energy	Internal energy
1	−2.145	−14.850	−16.985	1.150
2	−4.852	−31.47	−36.32	18.585
3	−0.435	−24.911	−25.346	1.876
4	−3.909	−37.297	−41.206	7.734
5	−2.695	−39.349	−42.044	30.708
6	−4.500	−37.716	−42.216	18.547

4. Conclusion

Herein, a lactam and five chiral amino alcohols derived from chiral 1,2-diaminocyclohexane have been designed for potential PTP1B inhibition. We have demonstrated that the regioselective ring opening reaction of (*R*)-styrene oxide by amine nucleophile and absolute configuration of desired product **2**–**4** could be assigned by their X-ray diffraction data. In the design of more effective medicines, the development of such molecules and targeting the surface residues, for example, the region containing Met258, Arg254, Gln102 and Asp29 of the second phosphate binding site, might be advantageous. Dock score analysis demonstrated that ligands **4**–**6** are potential inhibitors towards PTP1B by hydrogen bonds especially with Gln102 and Asp29 of the second phosphate binding site.

5. Experimental

5.1. Apparatus and chemicals

Melting points were determined with GALLENKAMP Model apparatus with open capillaries. Infrared spectra were recorded on a MİDAC-FTIR Model 1700 spectrophotometer. The Elemental analyses were obtained with CARLO-ERBA Model 1108 apparatus. Optical rotations were recorded using PERKIN ELMER Model 341 polarimeter. ^{1}H NMR (400 MHz) and ^{13}C NMR (100 MHz) spectra were recorded on BRUKER DPX-400 high performance digital FT-NMR spectrometer, with tetramethysilane as the internal standard solutions in deuteriochloroform.

5.2. *N,N′*-Dibenzyl-(1*R*,2*R*)-1,2-diaminocyclohexane 1

This compound was synthesized by a previous method[40,41] by using (1*R*,2*R*)-1,2-diaminocyclohexane (1.0 g, 8.77 mmol) to give 2.60 g, 99% of compound **1**. $[\alpha]_D^{20} = -79.7$ (*c* 2.5, $CHCl_3$) ^{1}H NMR ($CDCl_3$): (δ, ppm) 7.20–7.50(m, 10H), 3.98(d, 2H, *J* = 13.2 Hz), 3.75 (d, 2H, *J* = 13.2 Hz), 2.36 (m, 2H, *J* = 3.6), 2.24 (d, 2H, *J* = 13.2 Hz), 2.15 (br s, 2H), 1.81–1.85 (m, 2H), 1.30–1.36 (m, 2H), 1.10–1.15 (m, 2H). ^{13}C NMR ($CDCl_3$): δ (ppm) 141.01, 128.38, 128.19, 126.79, 60.90, 50.89, 31.56, 25.08.

5.3. *N,N′*-Dibenzyl-(*1R,2R*)-1,2-Diaminocyclohexaneoxalylamide 2

N,N′-Dibenzyl-(1*R*,2*R*)-1,2-diaminocyclohexane **1** (500 mg, 1.7 mmol) and oxalyl chloride (200 mg, 1.7 mmol) was refluxed in toluene (3 mL) under argon for 24 h. After evaporation of the solvent, the crude product was purified by flash column chromatography eluted with hexane/EtOH (9:1) to give 0.42 g (71%), mp 166–167 °C, $[\alpha]_D^{20} = +70.3$ (*c* 0.5, $CHCl_3$). IR (cm^{-1}): 3254, 3219, 3102, 3033, 2994, 2939, 2878, 1676, 1402, 1355, 1256, 1041, 810, 794, 771, 708, 665. ^{1}H NMR δ: 7.36–7.24 (m, 5H), 5.295 (d, 15.96 Hz, 1H); 4.55 (d, 15.96 Hz, 1H); 3.48–3.46 (m, 1H); 2.26–2.18 (m, 1H); 1.74–1.72 (m, 1H); 1.31–1.11 (m, 2H). ^{13}C NMR (δ, ppm): 158.66, 136.62, 128.83, 127.45, 127.11, 58.12, 45.59, 28.75, 23.80. Anal. Calcd. for $C_{23}H_{27}N_2O_{2.5}$ C: 74.29, H: 7.27, N: 7.53. Found; C: 74.73, H: 7.08, N: 7.32.

5.4. *N,N′*-Dibenzyl-*N,N′*-bis[(*S*)-2-hydroxy(2-phenyl)ethyl]-(1*R*,2*R*)-1,2-diaminocyclo-hexane 3

(*S*)-Styrene oxide (1.63 g, 13.6 mmol) was added to a solution of *N,N′*-Dibenzyl-(1*R*,2*R*)-1,2-diaminocyclohexane **1** (2 g, 6.8 mmol) in methanol (3 mL) and stirred at 40, 50 and 60 °C, for 24 h for each temperature. The solvent was evaporated and the remaining epoxide and amine were removed by Kugelrohr distillation apparatus. The crude product was purified by crystallization from *n*-hexane and ethanol to give **3** (2.72 g, 75%) as a white powder. Mp 202–203 °C; $[\alpha]_D^{20} = -147.6$ (*c* 1 $CHCl_3$). IR (ν: cm^{-1}): 3429, 3242, 3063, 3030, 2928, 2851, 1490, 1458, 1336, 1240, 1195, 1105, 1066, 1022, 758, 714 cm^{-1}; ^{1}H (400 MHz, $CDCl_3$) 7.71–7.07 (20H, m), 5.78 (2H, br s, OH), 5.02 (1H, br s), 4.73 (1H, br s), 4.0–3.50 (4H, m), 3.19–2.55 (6H, m), 2.23–1.69 (4H, m), 1.28–1.23 (4H, m). ^{13}C (100 MHz, $CDCl_3$):

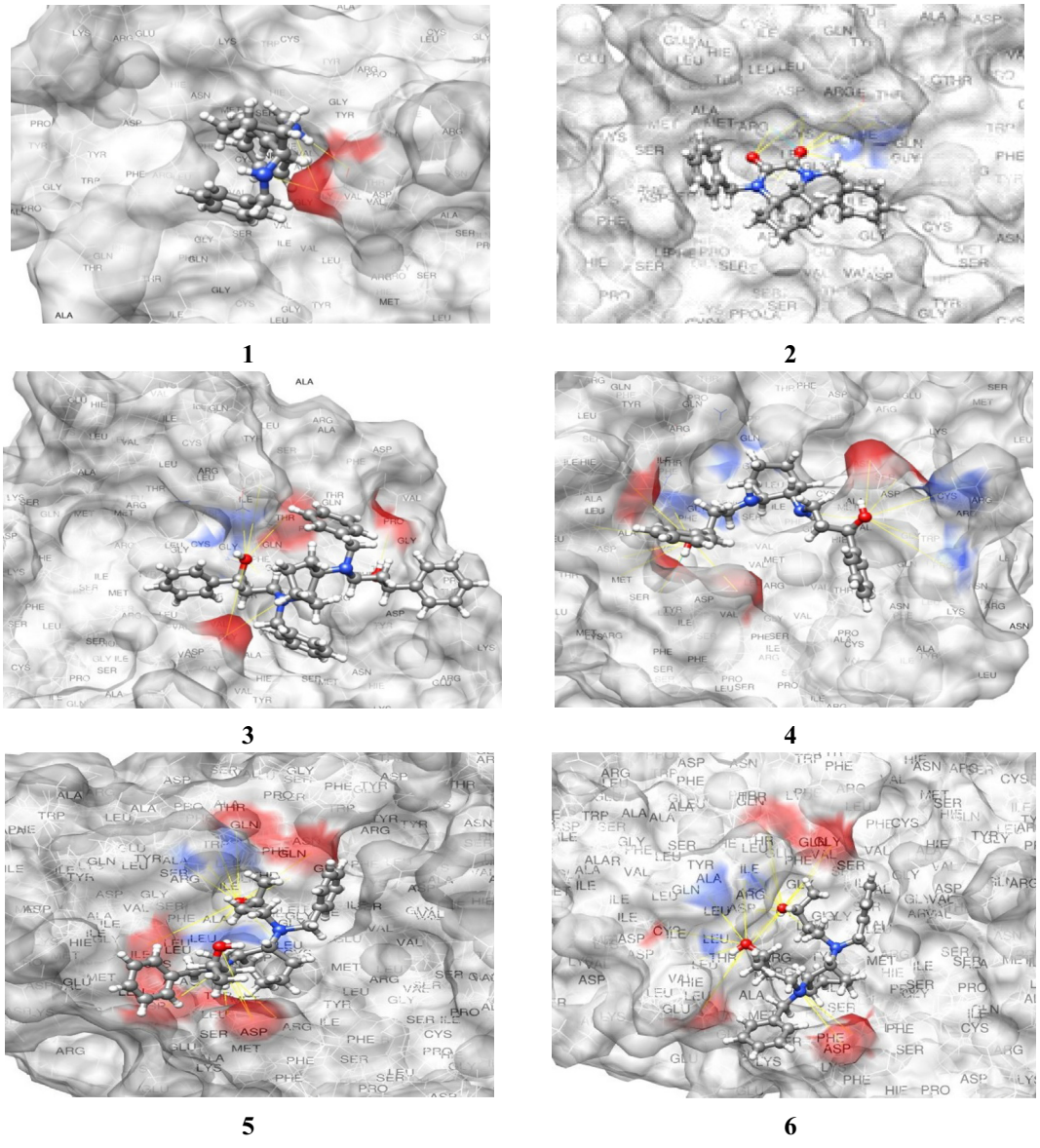

Figure 6. The orientation of the residues shown as sticks around inhibitor compounds in the final snophot of Dock result.

Table 3
Calculated Lipinski parameters for complexation of ligands **1**–**6** by Molinspiration method

Ligand	LogP	Mw	*n*ON	*n*OHNH	*n*Rotb
1	4.07	294	2	2	6
2	3.06	348	4	0	4
3	6.16	534	4	2	12
4	2.90	354	4	4	8
5	4.02	430	4	2	10
6	0.73	230	4	4	6

LogP: octanol/water partition coefficient, Mw: molecular weight, *n*ON: number of hydrogen bond acceptors, *n*OHNH: number of hydrogen bond donors, *n*Rotb: number of rotatable bonds.

143.23, 138.39, 130.55, 130.08, 128.43, 127.27, 126.01, 76.80, 72.27, 69.02, 58.43, 25.69, 24.27. Anal. Calcd. for $C_{36}H_{42}N_2O_2$: C, 80.89; H, 7.86; N, 5.24, Found: C, 80.25; H, 7.46; N, 5.30.

5.5. *N,N*′-Bis[(*S*)-2-hydroxy(2-phenyl)ethyl]-(1*R*,2*R*)-1,2-diaminocyclohexane 4

At first, $Pd(OH)_2$/C (20%, 75 mg) was added in one portion to a solution of the appropriate compound (1*R*,2*R*)-*N*,*N*′-dibenzyl-bis[(*S*)-2-hydroxy-(2-phenyl)ethyl]-1,2-diaminocyclohexane (400 mg, 0.75 mmol) in methanol (2 mL) as described.[44] The mixture was stirred under hydrogen and the reaction was monitored by TLC. After completion of the reaction, sodium carbonate (80 mg, 0.75 mmol) was added and stirred for 1 h. The solution was filtered and washed with methanol, then concentrated in vacuo. The crude product was purified by flash chromatography on silica gel H/EA/EtOH/TEA (4:1:1:0.5 as eluent) to give 186 mg % 70.05 of compound **2** as a viscous oil. Diastereomer single

crystals could be obtained from this oil by dissolving *n*-hexane and ethanol. IR (cm^{-1}): 3346, 3250, 3057, 3030, 2926, 2860, 1493, 1453, 1348, 1310, 1195, 1139, 1056, 924, 893, 854, 791, 756, 701. ^1H NMR ($CDCl_3$) δ: 7.41–7.27 (m, 10H), 4.55 (dd, 4, 8.12 Hz, 2H), 2.90–2.71 (m, 8H), 2.32–2.27 (m, 2H), 2.12–1.99 (m, 2H), 1.38–1.37 (m, 2H); 1.28–1.05 (m, 4H). ^{13}C NMR ($CDCl_3$): 142.55, 128.39, 127.48, 125.90, 72.00, 60.32, 53.84, 31.87, 25.01. Anal. Calcd for $C_{22}H_{30}N_2O_2$ C, 74.57; H, 8.47; N, 7.90. Found: C, 74.86; H, 8.34; N, 7.79.

5.6. *N,N′*-Dibenzyl-*N,N′*-di[(*S*)-2-hydroxypropyl]-(1*R*,2*R*)-diaminocyclohexane 5

(*S*)-Propylene oxide (118 mg, 2.0 mmol) was added to a solution of *N,N′*-Dibenzyl-(1*R*,2*R*)-1,2-diaminocyclohexane **1** (250 mg, 0.82 mmol) in methanol (3 mL) and stirred at 40 °C for 24 h, and 50 °C for 24 h as described.[41] The solvent was evaporated to give a pure product (340 mg, 99%). IR: *ν* 3384, 3031, 2923, 2858, 1953, 1600, 1452, 1296, 1388, 1336, 1253, 1132, 1060, 964, 746 cm^{-1}. ^1H NMR ($CDCl_3$): δ (ppm) 7.36–7.15(m, 10H), 5.92 (br s, 2H), 3.74 (d, 2H, J = 12.8 Hz), 3.49–3.40 (m, 4H), 2.70–2.60 (m, 4H), 2.40–2.34 (m, 2H), 2.00–1.90 (m, 2H), 1.80–1.60 (m, 2H), 1.20–0.9 (m, 10H); ^{13}C NMR ($CDCl_3$): δ (ppm) 139.78, 129.61, 128.23, 127.21, 65.89, 64.31, 59.83, 56.92, 25.97, 25.03, 21.78. Anal. Calcd for $C_{26}H_{38}N_2O_2$: C, 76.09; H, 9.27; N, 6.83. Found: C, 75.92; H, 9.12; N, 6.34.

5.7. X-ray experimental part

The diffraction data were measured at low temperature on various diffractometers. The datasets were reduced by EvalCCD,[45] [28], *automar* [29],[46] *Crysalis PRO* [30][47] and then corrected for absorption.[48]

The solutions and refinements were performed by SHELX.[49] The crystal structures were refined using full-matrix least-squares based on F^2 with all non hydrogen atoms anisotropically defined. Hydrogen atoms were placed in calculated positions by means of the 'riding' model. More details concerning the refinement of the crystal structures are shown in Table 1. The CCDC reference number of crystals 2, 3 and 4 is 1463691, 1463692, 1463693 respectively. Crystallographic data can be obtained free of charge via http://www.ccdc.cam.ac.uk/conts/retrieving.html (or from the Cambridge Crystallographic Data Centre, 12, Union Road, Cambridge CB21EZ, UK; fax: + 44 1223 336 033; deposit@ccdc.cam.ac.uk).

References

1. Tonks, N. K. *FEBS Lett.* **2003**, *546*, 140–148.
2. (a) Saltiel, A. R.; Kahn, C. R. *Nature* **2001**, *414*, 799–806; (b) Evans, J. L.; Jallal, B. *Expert Opin. Invest. Drugs* **1999**, *8*, 139–160.
3. (a) Cheng, A.; Dube, N.; Gu, F.; Tremblay, M. L. *Eur. J. Biochem.* **2002**, *269*, 1050–1059; (b) Zhang, Z.; Lee, S. Y. *Expert Opin. Invest. Drugs* **2003**, *12*, 223–233.
4. Thareja, S.; Aggarwal, S.; Bhardwaj, T. R. *Med. Res. Rev.* **2010**. https://doi.org/10.1002/med.20119.
5. Zhang, S.; Zhang, Z. Y. *Drug Discovery Nat. Rev.* **2007**, *12*, 9–10.
6. Bharatham, K.; Bharatham, N.; Kwon, Y. J.; Lee, K. W. *J. Comput. Aided Mol. Des.* **2008**, *12*, 925–933.
7. Wang, J.; Chan, S. L.; Ramnarayan, K. J. *Comput. Aided. Mol. Des.* **2003**, *8*, 495–513.
8. Jr Burke, T. R.; Zhang, Z. Y. *Biopolymers* **1998**, *47*, 225–241.
9. Liu, G.; Tan, J.; Niu, C.; Shen, J.; Luo, X.; Shen, X.; Chen, K.; Jiang, H. *Acta Pharm. Sin.* **2006**, *27*, 100–110.
10. Zabell, A. P. R.; Corden, S.; Helquist, P.; Stauffacher, C. V.; Wiest, O. *Bioorg. Med. Chem.* **2004**, *12*, 1867–1880.
11. Huang, P.; Ramphal, J.; Wei, J.; Liang, C.; Jallal, B.; McMahon, G.; Tang, C. *Bioorg. Med. Chem.* **2003**, *11*, 1835–1849.
12. Murthy, V. S.; Kulkarni, V. M. *Bioorg. Med. Chem.* **2002**, *10*, 897–906.
13. Burke, T. R., Jr.; Ye, B.; Yan, X.; Wang, S.; Jia, Z.; Chen, L.; Zhang, Z. Y.; Barford, D. *Biochemistry* **1996**, *35*, 15989–15996.
14. Moretto, A. F.; Kirincich, S. J.; Xu, W. X.; Smith, M. J.; Wan, Z. K.; Wilson, P.; Follows, B. C.; Binnun, E.; Joseph-McCarthy, D.; Foreman, K.; Erbe, D. V.; Zhang, Y. L.; Tam, S. K.; Tam, S. Y.; Lee, J. *Bioorg. Med. Chem.* **2006**, *14*, 2162–2177.
15. Kumar, R.; Shinde, R. N.; Ajay, D.; Sobhia, M. E. *J. Chem. Inf. Model.* **2010**, *50*, 1147–1158.
16. Sun, L.-P.; Ma, W.-P.; Gao, L.-X.; Yang, L.-L.; Quan, Y.-C.; Li, J.; Piao, H.-R. *J. Enzyme Inhib. Med. Chem.* **2013**, *2*, 1199–1204.
17. Bamane, R. V.; Chitre, T. S.; Rakholiya, V. K. *Der Pharma Chemica* **2011**, *3*, 227–237.
18. Dixit, M.; Saeed, U.; Kumar, A.; Siddiqi, M. I.; Tamrakar, A. K.; Srivastava, A. K.; Goel, A. *Med. Chem.* **2008**, *4*, 18–24.
19. Sun, S.-X.; Li, X.-B.; Liu, W.-B.; Ma, Y.; Wang, R.-L.; Cheng, X.-C.; Wang, S.-Q.; Liu, W. *Int. J. Mol. Sci.* **2013**, *14*, 12661–12674.
20. Jiang, C.-S. *J. Asian Nat. Prod. Res.* **2017**. https://doi.org/10.1080/10286020.2017.1317752.
21. Chandrashekhar, L. A.; Chandrashekhar, D. U. *Int. J. Pharm. Phytopharmacol. Res.* **2014**, *3*, 383–386.
22. Ottanàa, R.; Maccaria, R.; Ciurleoa, R.; Paolib, P.; Jacomellib, M.; Manaob, G.; Camicib, G.; Laggnerc, C.; Langerd, T. *Bioorg. Med. Chem.* **2009**, *17*, 1928–1937.
23. Basu, S.; Prathipati, P.; Thorat, S.; Ansari, S.; Patel, M.; Jain, V.; Niranjan, S.; De, S.; Reddy, S. *Bioorg. Med. Chem.* **2017**, *25*, 67–74.
24. Evans, D. A.; Seidel, D. *J. Am. Chem. Soc.* **2005**, *127*, 9958–9959.
25. Evans, D. A.; Mito, S.; Seidel, D. *J. Am. Chem. Soc.* **2007**, *1291*, 1583–11592.
26. Cooper, C. J.; Jones, M. D.; Brayshaw, S. K.; Sonnex, B.; Russel, M. L.; Mahona, M. F.; Allan, D. R. *Dalton Trans.* **2011**, *40*, 3677–3682.
27. Ager, D. J.; Prakash, I.; Schaad, D. R. *Chem. Rev.* **1996**, *96*, 835–875.
28. Fache, F.; Schulz, E.; Tommasino, M. L.; Lemaire, M. *Chem. Rev.* **2000**, *100*, 2159–2231.
29. Bergmeier, S. C. *Tetrahedron* **2000**, *56*, 2561–2576.
30. Gnas, Y.; Glorius, F. *Synthesis* **2006**, *12*, 1899–1930.
31. Pradeep, C. P.; Das, S. K. *Coord. Chem. Rev.* **2013**, *257*, 1699–1715.
32. Thomas, C.; Brut, S.; Bibal, B. *Tetrahedron* **2014**, *70*, 1646–1650.
33. Case, D. A.; Darden, T. A.; Cheatham Simmerling, C. L.; Wang, J.; Duke, R. E.; Luo, R.; Merz, K. M.; Pearlman, D. A.; Crowley, M.; Walker, R. C.; Zhang, W.; Wang, B.; Hayik, S.; Roitberg, A.; Seabra, G.; Wong, K. F;. Paesani, F.; Wu, X.; Brozell, S.; Tsui, V.; Gohlke, H.; Yang, L.; Tan, C.; Mongan, J.; Hornak, V.; Cui, G.; Beroza, P.; Mathews, D. H.; Schafmeister, C.; Ross, W. S.; Kollman, P. A., *Amber 9*, 2006.
34. Duan, Y.; Wu, C.; Chowdhury, S.; Lee, M. C.; Xiong, G. M.; Zhang, W.; Yang, R.; Cieplak, P.; Luo, R.; Lee, T.; Caldwell, J.; Wang, J. M.; Kollman, P. *J. Comput. Chem.* **2003**, *24*, 1999–2012.
35. Case, D. A.; Cheatham, T. E.; Darden, T.; Gohlke, H.; Luo, R.; Merz, K. M.; Onufriev, A.; Simmerling, C.; Wang, B.; Woods, R. J. *J. Comput. Chem.* **2005**, *26*, 1668–1688.
36. Bayly, C. I.; Cieplak, P.; Cornell, W. D.; Kollman, P. A. *J. Phys. Chem.* **1993**, *97*, 10269–10280.
37. Wang, J. M.; Wolf, R. M.; Caldwell, J. W.; Kollman, P. A.; Case, D. A. *J. Comput. Chem.* **2004**, *25*, 1157–1174.
38. Albano, V. G.; Bandini, M.; Melucci, M.; Monari, M.; Piccinelli, F.; Tommasi, S. *Adv. Synth. Catal.* **2005**, *347*, 1507–1512.
39. Srimurugan, S.; Viswanathan, B.; Varadarajan, T. K.; Varghese, B. *Tetrahedron Lett.* **2005**, *46*, 3151–3155.
40. Tye, H.; Eldred, C.; Wills, M. *Tetrahedron Lett.* **2001**, *43*, 155–159.
41. Karakaplan, M.; Ak, D.; Çolak, M.; Ozhan Kocakaya, Ş.; Hoşgören, H.; Pirinççioğlu, N. *Tetrahedron* **2013**, *69*, 349–358.
42. Lipinski, C. A.; Lombardo, F.; Dominy, B. W.; Feeney, P. J. *Adv. Drug. Delivery Rev.* **1997**, *23*, 4–25.
43. Veber, D. F.; Johnson, S. R.; Cheng, H. Y.; Smith, B. R.; Ward, K. W.; Kopple, K. D. *J. Med. Chem.* **2002**, *45*, 2615–2623.
44. Xua, X. H.; Qiu, X. L.; Qing, F. L. *Tetrahedron* **2008**, *64*, 7353–7361.
45. Duisenberg, A. J. M.; Kroon-Batenburg, L. M. J.; Schreurs, A. M. M. *J. Appl. Crystallogr.* **2003**, *36*, 220–229.
46. *Automar, release 2.8.0*, (2011) Marresearch. 1.171.35.21, 2012.
47. Blessing, R. H. *Acta Crystallogr., Sect. A* **1995**.
48. *Crysalis PRO*, Agilent Technologies, release. A 51:33–38.
49. Sheldrick, G. M. SHELX *Acta Crystallogr., Sect. A* **2008**, *64*, 112–122.